Struct Chem (2015) 26:685–693
DOI 10.1007/s11224-014-0504-5

ORIGINAL RESEARCH

Phenol interaction with different nano-cages with and without an electric field: a DFT study

Alireza Soltani · Mohammad T. Baei · Mohammad Ramezani Taghartapeh · E. Tazikeh Lemeski · Shamim Shojaee

Received: 26 May 2014 / Accepted: 25 August 2014 / Published online: 21 October 2014

Abstract The adsorption properties of the phenol molecule (C_6H_5OH) upon the outer surfaces of C_{24}, $B_{12}P_{12}$, $B_{12}N_{12}$, $Al_{12}N_{12}$, and $Al_{12}P_{12}$ were investigated using density functional theory calculations. Our calculations reveal that the phenol molecule can be chemisorbed on the sidewalls of $Al_{12}N_{12}$ and $Al_{12}P_{12}$ with adsorption energies of −1.03 and −0.76 eV, respectively. While the adsorption energy of C_6H_5OH on $Al_{12}N_{12}$ is typically more than that of $Al_{12}P_{12}$ cluster. We also considered the adsorption of the C_6H_5OH molecule under a strong electric field over $Al_{12}N_{12}$. The results indicate that $Al_{12}N_{12}$ has high sensitivity to the phenol molecule in the presence of an electric field.

Keywords Nano-cage · External electric field effect · Phenol · Chemical sensor

Introduction

Phenol (C_6H_5OH) or carbolic acid is a white crystalline solid which first extracted from coal tar while it is now produced on a large scale (about 7 billion kg year^{-1}) from petroleum. It is known as a key precursor for producing different materials including polycarbonates, epoxies, Bakelite, nylon, detergents, etc. Moreover, the adsorption of phenol is a fundamental set for the start of many catalytic reactions, resulting in the formation of a variety of products, such as bisphenol, phenolicresins, caprolactam, aniline, and alkylphenols. Its nature as a carcinogenic compound and high reactivity as a functional group on solid surfaces are two compelling reasons for phenol removal. Generally, repeated or prolonged exposure to phenolic compounds may have corrosive effects on the eyes, the skin, and the respiratory tract and may also cause dermatitis, or even second and third-degree burns. It can also cause various diseases including dysrhythmia, seizures, harmful effects on the liver and kidneys, etc. [1–4]. Hence, the phenol detection and removing processes are of the utmost importance for the human health, industrial, environmental, and energy applications [5–12]. The reason we carried out this work is not only to understand the adsorption phenomena of phenol upon C_{24}, $B_{12}P_{12}$, $B_{12}N_{12}$, $Al_{12}N_{12}$, and $Al_{12}P_{12}$ but also the impact of an electric field on the structural and electronic properties of the applied nano-cages interacted with phenol molecule. Although there are numerous studies focusing on the interaction energy and structural deformation of both the phenol molecule and adsorbents, there is still no report on the adsorption properties of the phenol molecule on the nano-cages. Some of the previous reports are as follows; Myers and Benziger have investigated the adsorption of the phenol molecule on the Ni (111) surface experimentally [13]. Experimental studies done by Xu and Ihm indicated that the O–H bond of the phenol can be effectively split on Rh and Pt surfaces [14, 15]. Theoretical studies by Zhao et al. [10] have shown that the OH group of the adsorbed phenol molecule can be split

A. Soltani (✉) · M. R. Taghartapeh
Young Researchers and Elite Club, Islamic Azad University, Gorgan Branch, Gorgan, Iran
e-mail: alireza.soltani46@yahoo.com

M. T. Baei
Department of Chemistry, Islamic Azad University, Azadshahr Branch, Azadshahr, Golestan, Iran

E. T. Lemeski
Department of Chemistry, Islamic Azad University, Gorgan Branch, Gorgan, Iran

S. Shojaee
Ischemic Disorders Research Center, Golestan University of Medical Sciences, Gorgan, Iran

on the SiNNT. Similar studies by Chakarova-Käck et al. [11] have shown that the phenol molecule adsorption on graphite (0001) and α-Al_2O_3 (0001) are energetically favorable. Abrams and co-workers have shown that phenol adsorption at the bridge site of the Ni (111) surface is the most energetically considerable [12]. In addition, they have studied the cleavage of O–H bond of phenol in the interaction with Ni surfaces [16]. Recently, several reports on $B_{12}N_{12}$, $B_{12}P_{12}$, and $Al_{12}P_{12}$, $Al_{12}N_{12}$ in interactions with different molecules are reported [17–21]. In particular, this work represents: (a) the adsorption phenomena of a single phenol upon C_{24}, $B_{12}P_{12}$, $B_{12}N_{12}$, $Al_{12}N_{12}$, and $Al_{12}P_{12}$; (b) the effect of an external electric field on the structural and electronic properties of the applied nano-cages.

Computational methods

In the present work, we considered the adsorption properties of the phenol molecule on the perfect C_{24}, $B_{12}N_{12}$, $B_{12}P_{12}$, $Al_{12}N_{12}$, and $Al_{12}P_{12}$ clusters. All the geometrical optimizations and energy calculations are performed using GAMASS program package [22] at the level of density functional theory (DFT) with B3LYP/6-311+G* basis set [23]. For full optimization of the applied systems, phenol molecule is allowed to move freely across the surface of clusters. The adsorption energy (E_a) of phenol molecule on the nano-cages is defined as follows:

$$E_a = E_{cluster-phenol} - (E_{cluster} + E_{phenol}), \quad (1)$$

where $E_{cluster-phenol}$ are the total energies of the adsorbent (phenol molecule) on the surfaces of adsorbents (C_{24}, $B_{12}N_{12}$, $B_{12}P_{12}$, $Al_{12}N_{12}$, and $Al_{12}P_{12}$). $E_{cluster}$ are the total energies of perfect C_{24}, $B_{12}N_{12}$, $B_{12}P_{12}$, $Al_{12}N_{12}$, and $Al_{12}P_{12}$. E_{phenol} is the total energy of a single phenol. Natural bond orbital (NBO) and density of states (DOSs) analyses were performed using DFT/B3LYP method with 6-311+G* basis set. The influence of the static electric field on the adsorption, structural, and electronic properties of phenol on the individual $Al_{12}N_{12}$ nano-cage were investigated. All the applied systems were fully relaxed and all atoms in the adsorbate and adsorbent were allowed to move freely during the optimization process. The static external electric field used separately at the positive X direction, which is perpendicular to X plan. The numerical values of the static electric field strengths in the X direction upon the $C_6H_5OH/Al_{12}N_{12}$ system is 200×10^{-4} a.u. (1 a.u. = 514.224 V nm^{-1}) [24]. It is observed that the influence of the static external electric field can be included by adding a field term in the Hamiltonian of the system; which has been verified by Farmanzadeh and Ghazanfary [24, 25]. The quantum molecular descriptors for the nano-cages were determined as follows:

$$\mu = -(I + A)/2 \quad (2)$$

$$\chi = -\mu \quad (3)$$

$$\eta = (I - A)/2 \quad (4)$$

$$S = 1/2\eta \quad (5)$$

$$\omega = (\mu^2/2\eta), \quad (6)$$

where I ($-E_{HOMO}$) is the ionization potential and A ($-E_{LUMO}$) is the electron affinity of the molecule. The electronegativity (χ) is determined as the negative of μ, where μ is the chemical potential of a system. Furthermore, hardness (η) can be approximated using the Koopmans' theorem. The electrophilicity index (ω) as defined by Parr et al. is given by Eq. 6 [26–29]. Fermi level (E_F) in a molecule (at $T = 0$ K) almost accommodates at the middle of the HOMO/LUMO energy gap (E_g). Indeed, what lies in the middle of the E_g is the chemical potential, then the Fermi level of the considered systems is at the center of the E_g when the Fermi level equals to the chemical potential of a free gas of electrons [30].

Results and discussion

Adsorption of phenol molecule on the nano-cages

First, we studied the reaction of a single phenol molecule (C_6H_5OH) on the outer sidewalls of pure C_{24}, $B_{12}P_{12}$, $B_{12}N_{12}$, $Al_{12}N_{12}$, and $Al_{12}P_{12}$ calculating the phenol molecule adsorption energies on these clusters. Figure 1 demonstrates the optimized structures of the phenol molecule adsorbed upon the pure C_{24} and $B_{12}P_{12}$ clusters.

The C–C, B–P, B–N, Al–P, and Al–N bond lengths in the perfect C_{24}, $B_{12}P_{12}$, $B_{12}N_{12}$, $Al_{12}P_{12}$, and $Al_{12}N_{12}$ are 1.49, 1.93, 1.48, 2.34, and 1.86 Å, respectively. The adsorption energies in the most stable configurations of an isolated phenol molecule adsorbed upon C_{24} and $B_{12}P_{12}$ are about −0.06 and −0.09 eV in the models **A** and **B**, respectively, indicating a weak physical adsorption upon these clusters owing to weak van der Waals interaction between the phenol and C_{24} and $B_{12}P_{12}$ nano-cages [16]. Since the DFT formalism employed in this work does not include Van der Waals effects, both the adsorption energies and the adsorption distances are to be considered as tentative. The average distances between phenol molecule and clusters are about 2.62 and 2.66 Å, respectively (see Fig. 1). The energies of phenol adsorption upon the walls of $B_{12}N_{12}$, $Al_{12}P_{12}$, and $Al_{12}N_{12}$ are in the range of −0.43, −0.76, and −1.03 eV in the models **A**, **B**, and **C**, respectively. The distance between the C_6H_5OH and the clusters (**A**, **B**, and **C**) are 1.71, 2.03, and 1.97 Å, respectively (Fig. 2), which primarily indicate for chemisorption. The results of the adsorption energy reveal

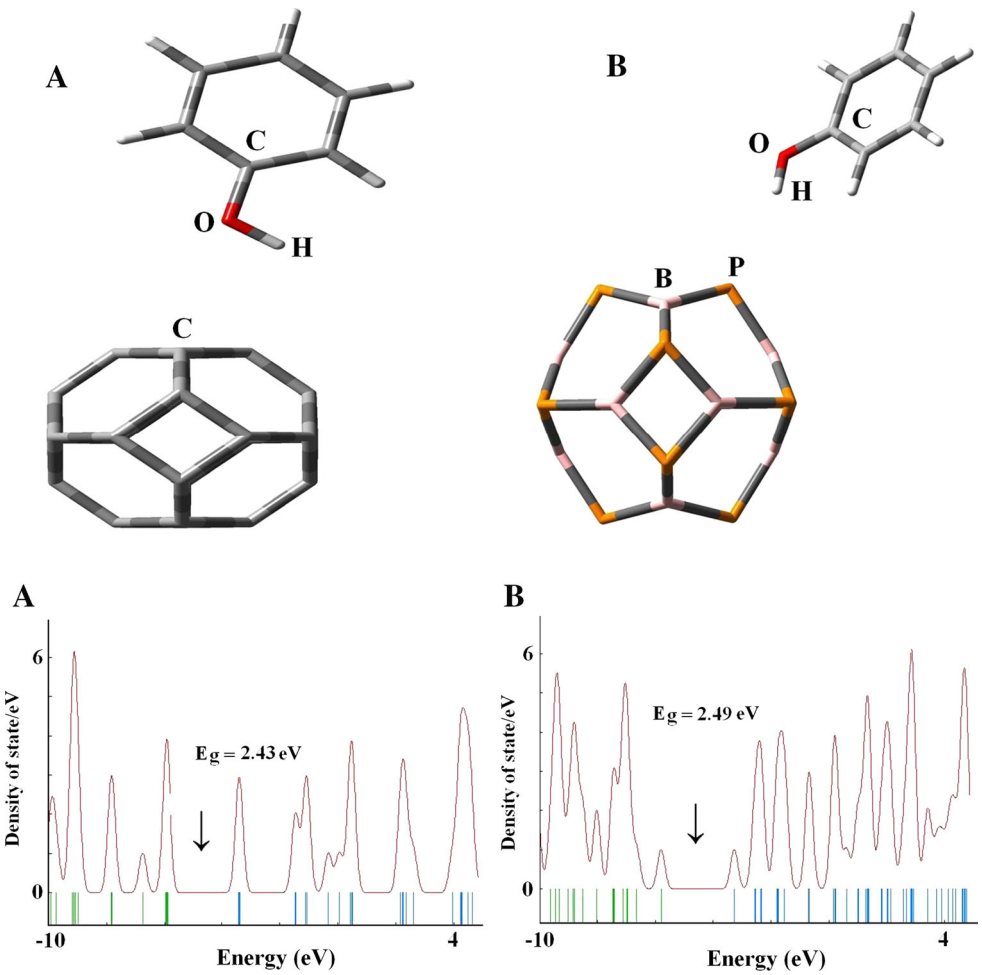

Fig. 1 The adsorption models and the density of states for C_6H_5OH interacted with **a** C_{24} and **b** $B_{12}P_{12}$ nano-cages

that $Al_{12}N_{12}$ is energetically more stable than $Al_{12}P_{12}$ nano-cage.

The influence of the phenol adsorption on $Al_{12}N_{12}$ and $Al_{12}P_{12}$ results in local structural deformations from sp^2 to sp^3 at the adsorption sites of nano-cages, where the Al atoms of nano-cages are slightly pulled out from the basic form. The computed adsorption energy of phenol molecule from hydroxyl head onto the wall of $Al_{12}N_{12}$ is expected to be larger in comparison to the phenol adsorption upon the surfaces of $C_{24} < B_{12}P_{12} < B_{12}N_{12} < Al_{12}P_{12}$. Therefore, we can deduce that the hydroxyl groups of C_6H_5OH are physisorbed upon the C_{24} and $B_{12}P_{12}$ being weakly bounded. In contrast, the phenol molecule onto the $B_{12}N_{12}$, $Al_{12}P_{12}$, and $Al_{12}N_{12}$ are chemically bounded, respectively. The bond lengths of C–C, B–P, B–N, Al–N, and Al–P are increased to 1.50, 1.54, 1.94, 1.91, and 2.39 Å, after the phenol adsorption on C_{24}, $B_{12}P_{12}$, $B_{12}N_{12}$, $Al_{12}N_{12}$ and $Al_{12}P_{12}$, respectively. The N–B–N, P–B–P, N–Al–N, and P–Al–P bond angles of these clusters are changed from 98.17°, 98.88°, 98.88°, and 94.60° before the adsorption processes to 94.12°, 98.61°, 92.50°, and 97.87° after the adsorption processes, respectively, preferring sp^3 hybridization. These results indicate a structural deformation due to the significant changes in properties such as adsorption energy, energy gap, and charge transfer. After the adsorption of phenol on C_{24}, $B_{12}P_{12}$, $B_{12}N_{12}$, $Al_{12}P_{12}$, and $Al_{12}N_{12}$ nano-cages, the O–H bond length of phenol is increased from 0.969 Å to 0.970, 0.973, 0.974, 0.975, and 0.986 Å, respectively. Larsen et al. [24] have experimentally showed that the O–H bond length of phenol molecule is 0.9574 Å. This experimental data is in good agreement with our study (0.969 Å).

It is found that the adsorption energy of phenol molecule on the nano-cages is increased with the decrease in the O–H distance [23]. Baei et al. [10] recently reported the adsorption of phenol molecule on the perfect, Ga-, In-doped (4,4)-BNNT surfaces with adsorption energies of −0.19, −1.18, and −0.93 eV, respectively. Chakarova-Käck and co-workers [24] also studied the adsorption of phenol on graphite and alumina with adsorption energies about 0.06 and 1.00 eV with the distances of 4.19 and 1.95 Å between two species at the PW91, respectively. Thierfelder

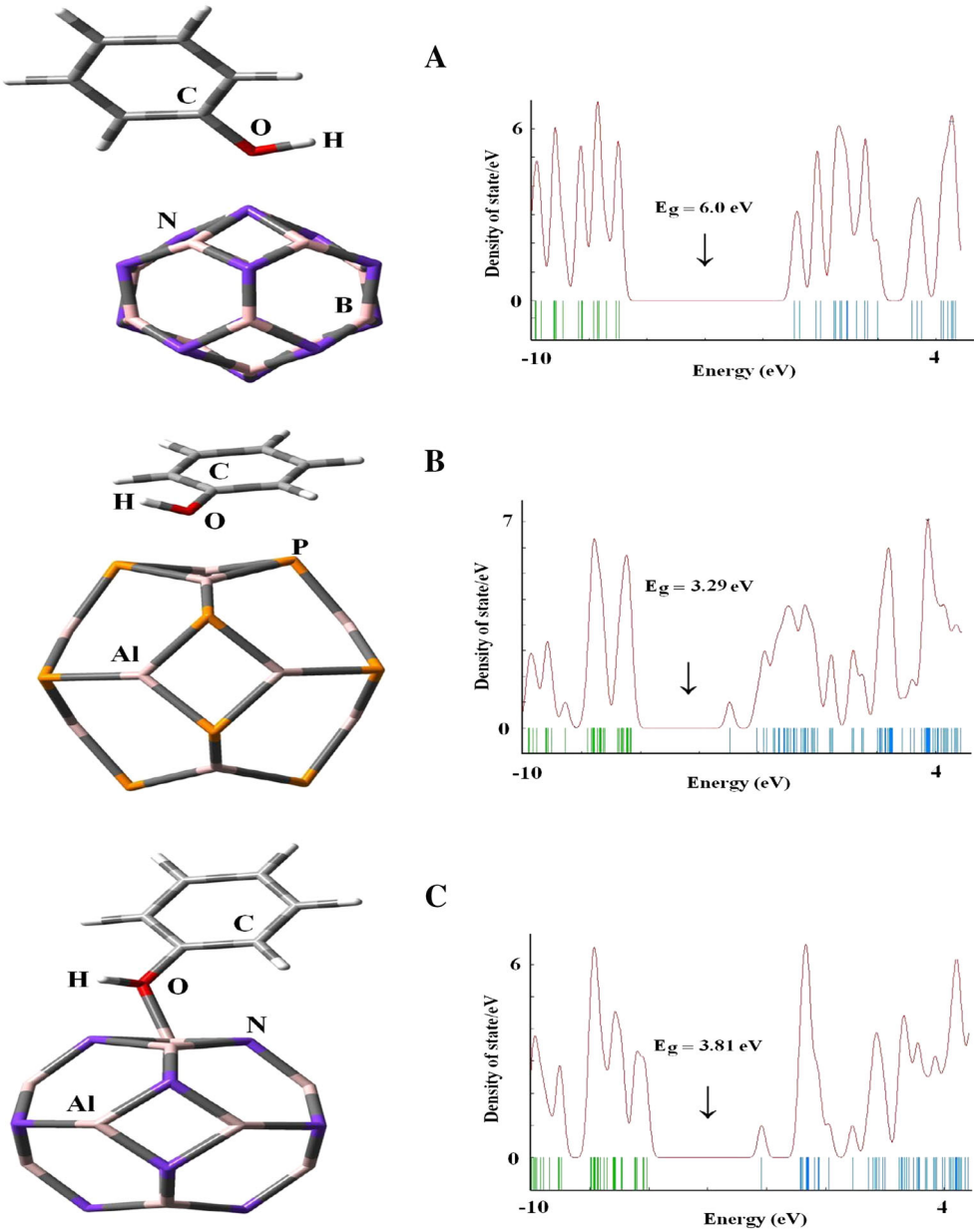

Fig. 2 The adsorption configurations and the density of states for C_6H_5OH interacted with **a** $B_{12}N_{12}$, **b** $Al_{12}P_{12}$, and **c** $Al_{12}N_{12}$ nano-cages

and co-workers [27] also reported methane adsorption on graphene with the adsorption energy about −0.17 eV using DFT calculations. Ahmadi and co-workers [21] represent that the interactions of BN, AlP, BP, and AlN nanotubes to CO molecule are about −0.02, −0.29, −0.31, and −0.34 eV at the B3LYP/6-311+G* level of theory, respectively.

To understand the adsorption properties of C_6H_5OH for the most stable configuration in $Al_{12}N_{12}$, the frontier molecular orbital (FMO) is calculated in Fig. 3. The highest occupied molecular orbital (HOMO) at the valence bond of phenol/$Al_{12}N_{12}$ complex is located more upon the nitrogen atom of cluster with energy about −6.06 eV, while the lowest unoccupied molecular orbital (LUMO) at the conduction bond of phenol/$Al_{12}N_{12}$ complex is located more onto the Aland N atoms of cluster and is slightly on the oxygen atom of phenol molecule with energy about −2.17 eV.

$Al_{12}N_{12}$ is a wide energy gap semiconductor with an energy gap of 3.85 eV, represents good dielectric properties, high thermal conductivity, and low thermal expansion coefficient [9]. The energy gap (E_g) of $Al_{12}N_{12}/C_6H_5OH$ is declined from 3.85 to 3.81 eV, as shown in Table 2. The DOS analysis shows that the phenol adsorption has not significant effect upon the electronic property of $Al_{12}N_{12}$ nano-cage.

NBO analysis for the $Al_{12}N_{12}/C_6H_5OH$ complex indicates that the net charge transfer from phenol to nano-cage

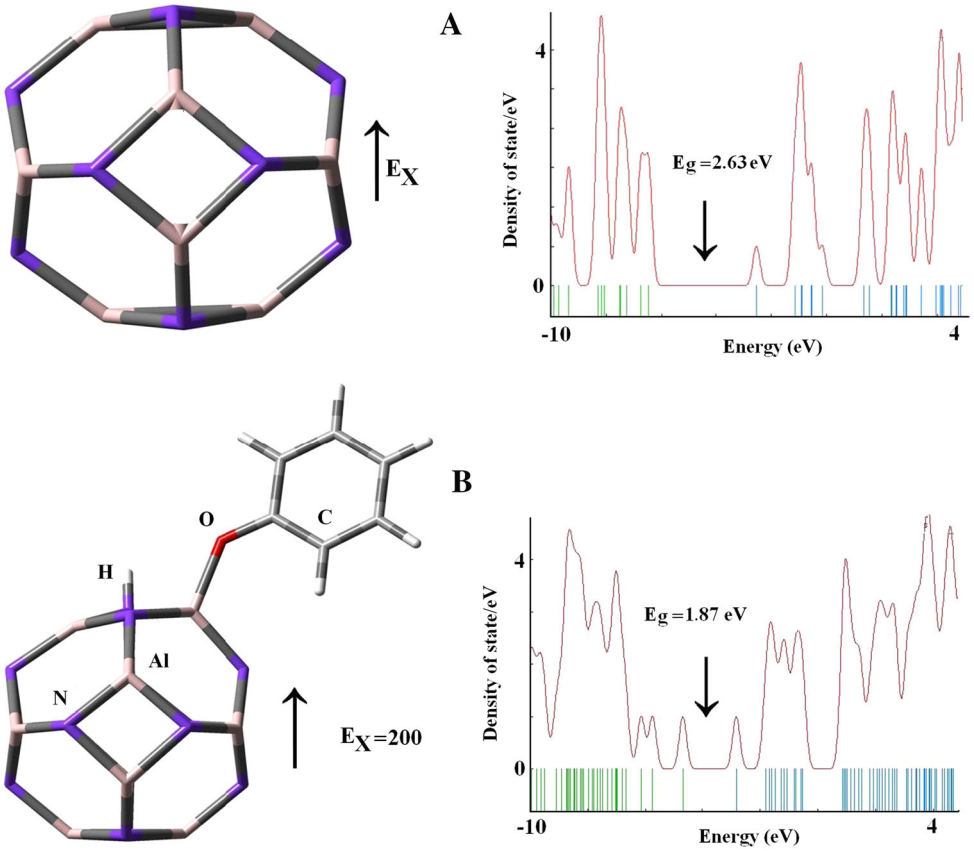

Fig. 3 The optimized structures of and the density of states for pure nano-cage (**a**) and phenol molecule interacted with $Al_{12}N_{12}$ with an electric field (**b**)

is about 0.11 el. The charge analysis demonstrates that the bonding character of the Al atom is changed from sp^2 to sp^3 with a charge transfer from phenol molecule to the anti-bonding orbitals of two Al–N bonds in the $Al_{12}N_{12}$ nano-cage. To further study of the adsorption behavior of phenol molecule upon the electronic structure of nano-cages, we analyzed the DOSs for phenol adsorption on C_{24}, $B_{12}P_{12}$, $B_{12}N_{12}$, $Al_{12}P_{12}$, and $Al_{12}N_{12}$ surfaces (Figs. 1, 2). The results indicate that the DOS near the Fermi level is not affected via the phenol adsorption for the most stable state on the wall of $Al_{12}N_{12}$. Hence, the Fermi levels of pristine $B_{12}N_{12}$, $Al_{12}N_{12}$, and $Al_{12}P_{12}$ changes from −4.39, −4.55, and −5.10 to −3.98, −4.11, and −4.64 eV for C_6H_5OH on $B_{12}N_{12}$, $Al_{12}N_{12}$, and $Al_{12}P_{12}$ complexes, respectively (see Table 1). These results indicate that a moderate hybridization has occurred for all systems. We also explore the adsorption properties of phenol molecule on the exterior wall of $Al_{12}N_{12}$ (the most stable configuration) using an external electric field of 200×10^{-4} a.u. ($E_X = 200$). Under the electric field, the values of interaction distance, geometric structure, and adsorption energy have very large differences. In the most stable configuration, the Al–N bond length of the pure $Al_{12}N_{12}$ changes from 1.89 Å at the zero field strength ($E_X = 0$) to 2.08 Å at the field strength of 200×10^{-4} a.u. ($E_X = 200$) for $C_6H_5OH/Al_{12}N_{12}$ complex. The bond angles of Al–N–Al and N–Al–N are changed from 86.5° and 95.5° in the perfect $Al_{12}N_{12}$ to 93.2° and 88.4° for the phenol adsorbed upon $Al_{12}N_{12}$ nano-cage at field strength of 200×10^{-4} a.u. (see Fig. 4). Under an electric field, the C–O and O–H bond lengths for pure phenol increased to 1.369 and 0.968 Å, respectively. Whereas for $C_6H_5OH/Al_{12}N_{12}$ complex in the presence of an electric field, the C–O and N–H bond lengths are about 1.322 and 1.02 Å, respectively. The average values of the C–C bond, near the –OH group of C_6H_5OH, has a

Table 1 The obtained structural parameters for phenol molecule adsorbed on various nano-cages

Property	*d* (O–H) (Å)	*d* (C–O) (Å)	*d* (C–C) (Å)	C–O–H (°)
C_6H_5OH	0.969	1.369	1.399	108.86
C_{24}/C_6H_5OH	0.970	1.368	1.399	109.73
$B_{12}N_{12}/C_6H_5OH$	0.974	1.417	1.388	111.55
$B_{12}P_{12}/C_6H_5OH$	0.973	1.366	1.399	109.67
$Al_{12}N_{12}/C_6H_5OH$	0.986	1.418	1.390	114.33
$Al_{12}P_{12}/C_6H_5OH$	0.975	1.416	1.389	112.83
$Al_{12}N_{12}/C_6H_5OH$ (E_X)	–	1.322	1.419	–
Expt., Ref. [11]	0.957	1.374	1.393	108.7

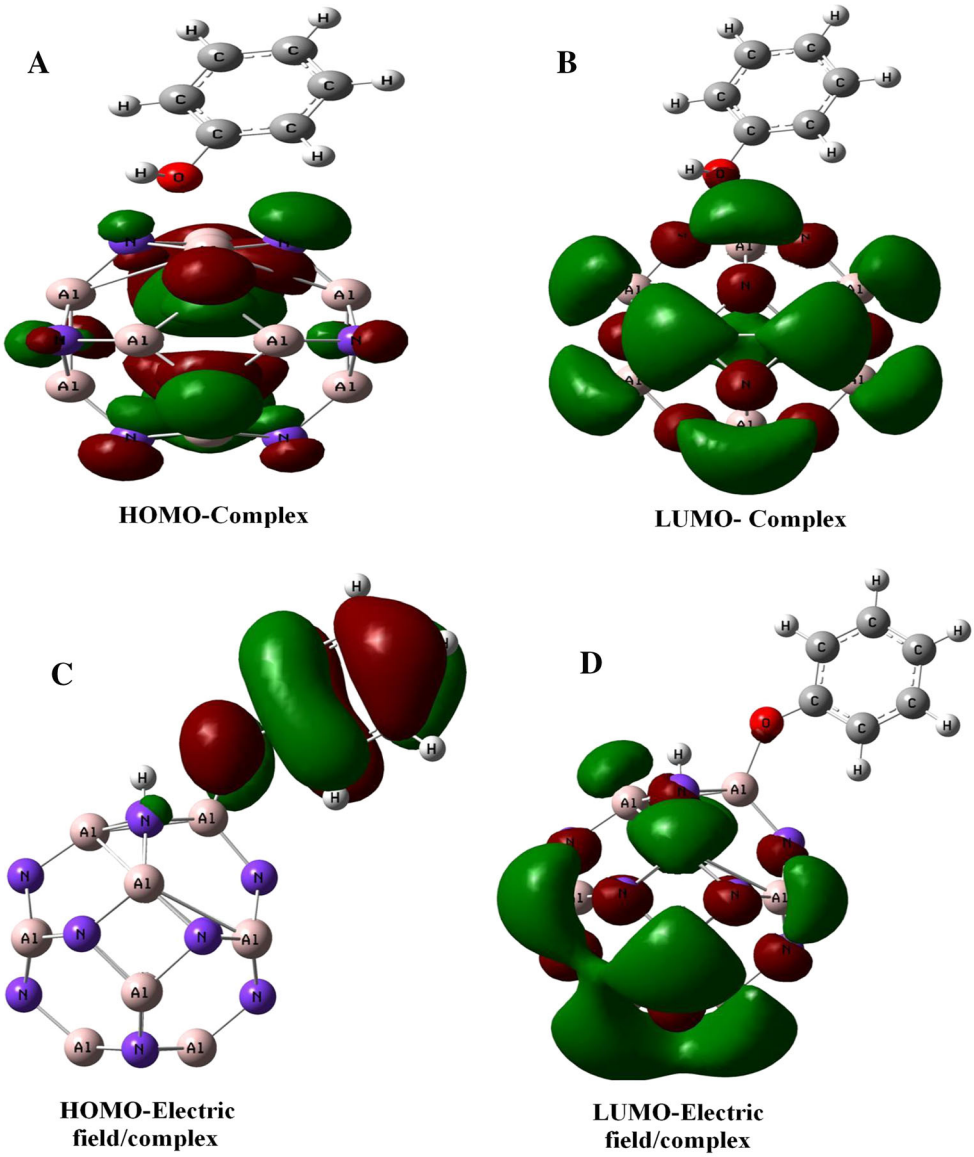

Fig. 4 The HOMO and LUMO for an isolated C_6H_5OH molecule, an isolated $Al_{12}N_{12}$, and the interaction of C_6H_5OH with $Al_{12}N_{12}$ nano-cage at the absence (**a**, **b**) and presence (**c**, **d**) of an electric field

negligible change about 1.40 Å in the pure phenol and 1.42 Å in the $C_6H_5OH/Al_{12}N_{12}$ system ($E_X = 200$).

The adsorption energy and the interaction distance of phenol adsorbed on the nano-cage under the electric field are −3.16 eV and 1.58 Å, respectively, and about 0.29 el is transferred from C_6H_5OH to $Al_{12}N_{12}$ nano-cage. This large E_{ad} value and small interaction distance show that the phenol molecule undergoes strong chemical adsorption onto the $Al_{12}N_{12}$, which is mainly electrostatic in nature. The adsorption energy of (C_6H_5O–SiCNT) system calculated by Zhao et al. lies at −1.617 eV with the distance of 1.70 Å [23]. In $C_6H_5O/Al_{12}N_{12}$ system, NBO analysis reveals that the point charges on the oxygen atom of phenol and the aluminum atom of $Al_{12}N_{12}$ nano-cage are about −0.883 and 1.954 el while the point charge of the O atom in the pure phenol and Al atom of nano-cage are −0.686 and 1.856 el, respectively, at the presence of an electric field, suggesting a charge transfer from the molecule to nano-cage. The computed Gibbs free energy (ΔG_{ads}) for $C_6H_5O/Al_{12}N_{12}$ complex is −37.82 kcal mol^{-1}, indicating that this molecule is adsorbed spontaneously. This result indicates that the phenol adsorption under an electric field is thermodynamically notable. The recovery time (the time required for something to resume its former or normal condition or state) of $Al_{12}N_{12}$ for phenol molecule at room temperature was calculated according to the formula, $\tau = \upsilon_0^{-1} e^{(-E_{ads}/K_B T)}$, where T is temperature, K_B is the Boltzmann's constant (8.62×10^{-5} eV K^{-1}) and υ_0 is the attempt frequency. The results of very strong interaction between two species under an electric field introduce this nano-cage as a sensor that has high sensitivity to the presence of phenol molecule due to a longer recovery time.

Table 2 E_{HOMO} (eV), E_{LUMO} (eV), E_g (eV), D_M (Debye), E_F (eV), and the corresponding quantum molecular descriptors for C_6H_5OH interacted with the pristine $Al_{12}N_{12}$ and $Al_{12}P_{12}$ nano-cages and electric field affected $C_6H_5OH/Al_{12}N_{12}$ system

Property	C_6H_5OH	$Al_{12}N_{12}$	$Al_{12}P_{12}$	$C_6H_5OH/Al_{12}N_{12}$	$C_6H_5OH/Al_{12}P_{12}$	$C_6H_5OH/Al_{12}N_{12}(E_X)$
E_{HOMO} (eV)	−7.28	−6.48	−6.76	−6.06	−6.31	−4.70
E_{LUMO} (eV)	−1.30	−2.63	−3.42	−2.17	−2.98	−2.83
E_g (eV)	5.94	3.85	3.34	3.81	3.29	1.87
D_M (Debye)	1.35	0.00	0.00	5.65	7.64	27.62
E_F (eV)	−4.29	−4.55	−5.10	−4.11	−4.64	−3.76
$[I = -E_{HOMO}]$ (eV)	7.28	6.48	6.76	6.06	6.31	4.70
$[A = -E_{LUMO}]$ (eV)	1.30	2.63	3.42	2.17	2.98	2.83
$[\eta = (I - A)/2]$ (eV)	2.99	1.92	1.65	1.90	1.62	0.93
$[\mu = -(I + A)/2]$ (eV)	−4.29	−4.55	−5.10	−4.16	−4.69	−3.76
$[S = 1/2\eta]$ (eV^{-1})	0.17	0.26	0.30	0.27	0.31	0.53
$[\omega = \mu^2/2\eta]$ (eV)	3.08	5.39	7.88	4.55	6.79	7.58

The influence of the external electric field upon the electronic properties of the $C_6H_5OH/Al_{12}N_{12}$ system was also investigated. Under an electric field, DOS plots indicate that the phenol adsorption has notable effect on the electronic properties of $Al_{12}N_{12}$ so that the HOMO–LUMO energy gap (E_g) of the cluster has declined from 2.63 to 1.87 eV (in Fig. 3). The change of energy gap (ΔE_g) of $Al_{12}N_{12}$ onto the adsorption behavior of phenol molecule is about 0.76 eV. This result shows that decrease in the energy gap leads to higher electrical conductivity. Under an electric field (Fig. 4c, d), the HOMO of $Al_{12}N_{12}/C_6H_5OH$ system (with the energy about −4.7 eV) is more located upon the phenol and is slightly situated upon the nitrogen atom of cluster. The LUMO of this complex (with the energy about −2.83 eV) is located more toward the Al and N atoms of $Al_{12}N_{12}$ and is slightly situated on the O atom of phenol molecule. Upon this study (Fig. 4a, b), the HOMO energy of this complex increases from −6.06 eV without the electrical field to −4.7 eV with the electrical field, while the LUMO energy of this complex decreases from −2.17 eV in the absence of an electrical field to −2.83 eV in the presence of an electrical field, respectively (Fig. 3). Hence, the DOS analysis in Fig. 3 reveals the phenol O–H bond dissociation on $Al_{12}N_{12}$ nano-cage in the presence of the electric field. The electronic properties of the nano-cage have been changed significantly in comparison with the above results. Moreover, under this electric field, the DOS near the valance bond has a distinct change compared with that of the pure $Al_{12}N_{12}$ nano-cage, so that an electron state appears at energy level of −4.70 eV (see Table 2). The large difference in the Fermi level of $Al_{12}N_{12}$ increases from −5.59 to −3.76 eV in the $Al_{12}N_{12}/C_6H_5OH$ complex. The Fermi level of $Al_{12}N_{12}$ in the presence of an electric field is noticeably shifted to lower energy of −3.76 eV which is larger in comparison to the Fermi level shift in the absence of an electric field. As shown in Fig. 5, the calculated molecular electrostatic potential (MEP) maps demonstrate that the positive charge (blue color) is located on the phenol (–OH group) added to $Al_{12}N_{12}$ in the absence of the electric field. Whereas the interaction between two species represents that the negative charge (red color) is located on the –OH group of phenol in the presence of an electric field.

Electric dipole moment

The size and direction of the electric dipole moment vector are altered under an electrical field when a phenol molecule moves up on the sidewall of $Al_{12}N_{12}$ nano-cage. The results of the electric dipole moment (D_M) for single species and the most stable configurations of the considered complexes indicate that during phenol adsorption for all complexes, the electric dipole moment increases with electric field strength ($E_X = 200$). The values of dipole moment (μ_D) under an electric field in pure $Al_{12}N_{12}$ increases from 0.00 Debye without electric field ($E_X = 0$) to 19.13 Debye with electric field. Under an electric field, the dipole moment for the applied parallel electric field (E_X) changes from 19.13 Debye in the perfect $Al_{12}N_{12}$ to 27.62 Debye in the $Al_{12}N_{12}/C_6H_5OH$ complex. On the other hand, μ_X for the applied parallel electric field increased from 19.12 Debye for the $Al_{12}N_{12}$ to 26.31 Debye for the $Al_{12}N_{12}/C_6H_5OH$ complex. This result indicates that the polarity of the applied systems have undergone changes after the adsorption of phenol onto the wall of $Al_{12}N_{12}$ at the presence of an electric field.

Quantum molecular descriptors

The best definition for global hardness is resistance toward deformation in presence of an electric field whose field strength is directly proportional to the stability of the system. The global hardness of $Al_{12}N_{12}$ is reduced from 1.92 eV at the zero electric field to 1.51 eV at the field strength of 200×10^{-4} a.u. ($E_X = 200$). When a phenol adsorbed on

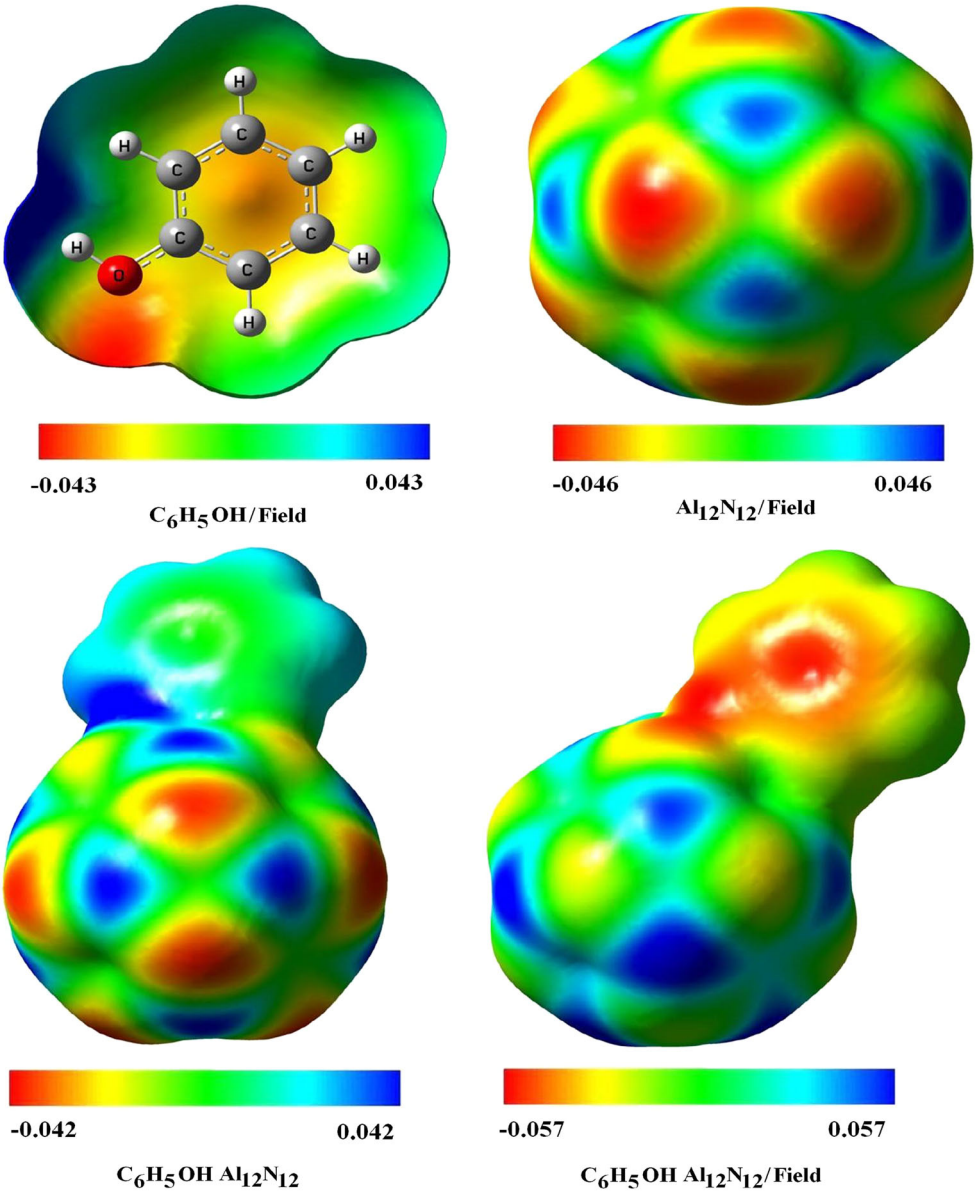

Fig. 5 MEP plots of phenol, pure $Al_{12}N_{12}$, and C_6H_5OH/$Al_{12}N_{12}$ complexes

the nano-cage in the presence and absence of an electric field, a decrease in global hardness leads to decrease in stability and increase in reactivity of the system [20]. Meanwhile, the chemical potential of cluster is declined from −4.55 eV at the zero electric field to −5.59 eV at the field strength of 200×10^{-4} a.u. ($E_X = 200$). The potential ionization (I) and electron affinity (A) of $Al_{12}N_{12}$ are gradually increased from 6.48 and 2.63 eV at the zero electric field to 6.92 and 4.34 eV at the field strength of 200×10^{-4} a.u., respectively. The global hardness of $Al_{12}N_{12}$ under the electric field diminishes from 1.51 to 1.11 eV for $Al_{12}N_{12}$/C_6H_5OH complex, with an increase in chemical potential from −5.59 eV in the pristine model to −3.76 eV in the $Al_{12}N_{12}$/C_6H_5OH complex, respectively. The stability of phenol adsorbed onto the wall of $Al_{12}N_{12}$ under an electric field is more notable than that without an electric field.

Conclusions

To summarize, we performed DFT calculations to explore the adsorption of phenol molecule on $Al_{12}N_{12}$. The results demonstrate that phenol molecule can be chemisorbed onto the sidewalls of $Al_{12}N_{12}$ and $Al_{12}P_{12}$, both with notable adsorption energies and charge transfer, which could induce notable changes in the structural properties of the clusters. We also found that the adsorption of C_6H_5OH/$Al_{12}N_{12}$ in the presence of an electric field is more significant than that without electric field, demonstrating that the $Al_{12}N_{12}$ cluster may be more suitable for the detection of C_6H_5OH molecule. The results reveal that the disassociation of H atom from the phenol molecule on the $Al_{12}N_{12}$ take place in the presence of an electric field, which is very useful to initiate some catalytic reactions. So, $Al_{12}N_{12}$ may

be a promising candidate for the detection of toxic phenol in the industrial applications.

Acknowledgments We would like to thank the Jaber Ebne Hayyan Unique Industry researchers Company. We should also thank the Nanotechnology Working Group of Young Researchers and Elite Club of Islamic Azad University, Gorgan Branch, Iran.

References

1. Wallace J (2005) Kirk-Othmer, encyclopedia of chemical technology, vol 18, 3rd edn. Wiley, New York, p 747
2. Budavari S (1996) The Merck Index: an encyclopedia of chemical, drugs, and biologicals. Merck, Whitehouse Station
3. Lin TM, Lee SS, Lai CS, Lin SD (2006) J Int Soc Burn Inj 32:517
4. Warner MA, Harper JV (1985) Anesthesiology 62:366
5. Hanscha C, McKarnsb SC, Smith CJ, Doolittle DJ (2000) Chem Biol Interact 127:61
6. Oku T, Hirano T, Kuno M, Kusunose T, Niihare K, Suganuma K (2000) Mater Sci Eng B 74:217
7. Oku T, Nishiwaki A, Narita I (2004) Sci Technol Adv Mater 5:635
8. Wang H (2010) Chin J Chem 28:1897
9. Sabirov DS, Bulgakov RG (2011) Comput Theor Chem 963:185
10. Zhao J-x, Gao B, Cai Q-h, Wang X-g, Wang X-z (2011) Theor Chem Acc 129:85
11. Chakarova-Käck SD, Øyvind B, Schröder E, Lundqvist BI (2006) Phys Rev B 74:155402
12. Delle Site L, Alavi A, Abrams CF (2003) Phys Rev B 67:193406
13. Myers AK, Benziger JB (1989) Langmuir 5:1270
14. Xu X, Friend CM (1989) J Phys Chem 93:8072
15. Ihm H, White JM (2000) J Phys Chem B 104:6202
16. Ghiringhelli LM, Caputo R, Delle Site L (2007) Phys Rev B 75:113403
17. Beheshtian J, Bagheri Z, Kamfiroozi M (2011) Microelectron J 42:1400
18. Ahmadi Phyghan A, Pashangpour M, Bagheri Z, Kamfiroozi M (2012) Physica E 44:1436
19. Beheshtian J, Kamfiroozi M, Bagheri Z, Ahmadi (2012) Comput Mater Sci 54:115
20. Beheshtian J, Peyghan AA, Bagheri Z (2012) Comput Mater Sci 62:71
21. Beheshtian J, Ahmadi Peyghan A, Bagheri Z, Kamfiroozi M (2012) Struct Chem 23:1567
22. Schmidt M, Baldridge K, Boatz J, Elbert S, Gordon M, Jensen J, Koseki S, Matsunaga N, Nguyen K, Su S, Windus T, Dupuis M (1993) J Comput Chem 14:1347
23. Beheshtian J, Baei MT, Ahmadi Peyghan A (2012) Surf Sci 606:981
24. Farmanzadeh D, Amirazami A (2009) Acta Phys Chim Sin 25:001
25. Farmanzadeh D, Ghazanfary S (2009) Struct Chem 20:709
26. Parr RG, Szentpaly L, Liu S (1999) J Am Chem Soc 121:1922
27. Parr RG, Pearson RG (1983) J Am Chem Soc 105:7512
28. Soltani A, Taghartapeh MR, Mighani H, Pahlevani AA, Mashkoor R (2012) Appl Surf Sci 259:637
29. Soltani A, Ahmadian N, Kanani Y, Dehno khalajid A, Mighani H (2012) Appl Surf Sci 258:9536
30. Baei MT, Ahmadi Peyghan A, Bagheri Z (2013) Solid State Commun 159:8